Left-handed and right-handed metamaterials composed of split ring resonators and strip wires

J. F. Woodley, M. S. Wheeler, and M. Mojahedi
Electromagnetics Group, Edward S. Rogers Sr. Department of Electrical and Computer Engineering, University of Toronto, Toronto, Canada M5S 2E4
(Received 21 December 2004; revised manuscript received 16 March 2005; published 13 June 2005)

The behavior of two structures composed of split ring resonators (SRRs) and strip wires (SWs) is examined through full wave simulations. It is shown that both structures exhibit a transmission peak in the region where the real parts of the electric permittivity and magnetic permeability are presumed to be negative, a property which is usually assumed to imply a negative index of refraction. However, an analysis of the dispersion characteristics and insertion phase of the two structures shows that the first structure, in which the SRRs and SWs are printed on opposite sides of a dielectric substrate, is a left-handed medium in the passband, whereas the second structure, in which SRRs and SWs are printed on the same side, is a right-handed medium in the passband. Hence the transmission magnitude alone does not provide sufficient evidence of a negative index of refraction. To determine the sign of the index correctly, the insertion phase for propagation through several lengths of the structure or calculations of dispersion diagrams are necessary. The impact of the unit cell size on the "handedness" of the structure is also examined.

DOI: 10.1103/PhysRevE.71.066605 PACS number(s): 41.20.Jb, 42.25.Bs, 03.65.Xp, 73.40.Gk

I. INTRODUCTION

In 1967 Veselago stated that a medium with negative real parts of the electric permittivity and magnetic permeability would have a negative real index of refraction [1]. In such a medium the electric field, the magnetic field, and the propagation vector $\vec{k}$ form a left-handed triplet. Because of this relationship, these media have been named left-handed media (LHM). Unfortunately, at the time, Veselago's predictions could not be corroborated experimentally, as suitable media with the required negative parameters were not available. It was not until three decades later that such media were developed.

In 1996 an array of metallic wires (SW) was shown to have a plasma frequency in the microwave regime [2]. Because of its low plasma frequency this structure can produce an effective negative permittivity at microwave frequencies while suffering relatively small losses. Then, in 1999 an array of split ring resonators (SRRs) was developed that exhibited a negative magnetic permeability in the resonance region [3]. The first negative index medium was developed soon after when these two structures were combined and it was shown that in the region where both the real parts of the electric permittivity and magnetic permeability were expected to be simultaneously negative a transmission passband and hence a peak in the transmission response appeared, implying the existence of the negative index of refraction [4]. The existence of a negative index in this medium was later corroborated by a refraction experiment in which an incoming wave was shown to refract negatively at the interface between this structure and air [5]. Since then, new LHM have been proposed and demonstrated experimentally [6–10]. Typically, in a structure composed of SRRs and strip wires (SW), in order to determine whether the given structure has a negative index of refraction or not, the transmission through the structure is measured and if a transmission peak is observed in the region where both the real parts of the permittivity and permeability are expected to be negative, then the structure is assumed to exhibit LHM behavior [4,7,11]. However, as will be discussed later, the emergence of a passband and a transmission peak is not sufficient evidence that the structure exhibits left handedness. In the case of SRR and SW, each of these elements when isolated produces the required negative behavior. However, when they are combined into a single structure their individual field patterns will interfere with one another. It is usually assumed that when these two elements are in close proximity their combined behavior does not deviate significantly from their isolated response, so that the correct "handedness" is still exhibited. As will be shown later, this interference can be significant enough to weaken or even destroy the LHM behavior, whereas still a passband and a transmission peak can be observed. In these situations, in order to correctly predict the left or right handedness, one must rely on other "diagnostic tools" such as calculating or measuring the *insertion phase and/or dispersion diagrams*.

This paper is organized as follows. In Sec. II we introduce two composite structures composed of SWs and SRRs and consider the transmission magnitude through these media. In Sec. III we determine the left or right handedness of these structures by considering the propagation phase through them. The dispersion diagrams of these structures will then be investigated in Sec. IV. In Sec. V the effects of the unit cell size on the handedness of one of the structures will be further investigated. Finally, Sec. VI summarizes our thoughts and provides some concluding remarks.

II. TRANSMISSION MAGNITUDE

In this paper we will consider two structures constructed by using SRRs and SWs printed on the same and opposite sides of a dielectric substrate. The dimensions of the rings in both structures were the same and are given in Fig. 1. The SWs were also identical for both structures. Figure 2 shows

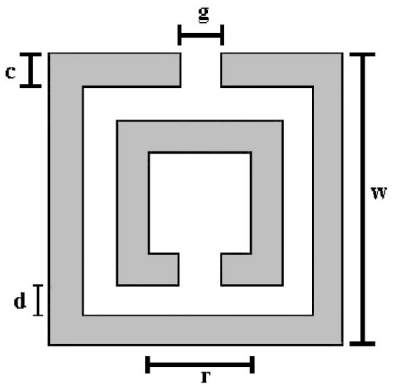

FIG. 1. Schematic of the split ring resonator. The dimensions used in the simulations were $r=0.506$ mm, $c=0.124$ mm, $d=0.15$ mm, and $g=0.114$ mm.

the two structures under consideration. In the first case the rings and strips are printed on opposite sides of the substrate [Fig. 2(a)] and in the second case the rings and strips are printed on the same side of the substrate [Fig. 2(b)]. We refer to these as the opposite side (OS) and same side (SS) structures, respectively.

The transmission through configurations such as above has been simulated and measured experimentally by many researchers [7,12,13]. In most cases where such structures have been considered—at frequencies where a simultaneous negative permittivity and permeability are expected to occur—a transmission peak has been observed, and hence it has been concluded that a negative index of refraction exists. But is the emergence of a passband and hence a transmission peak alone sufficient evidence that LHM behavior has occurred?

The transmission through the two SRR and SW configurations was simulated using Ansoft HFSS, a commercial full wave finite element simulation package. This package uses an iterative adaptive meshing technique[1] which divides the structure into a number of tetrahedra and then solves for the fields in these tetrahedra. The number of tetrahedra is then increased and the process is repeated in an iterative fashion until a desired convergence is achieved. The unit cells of the simulated structures are shown in Fig. 2. As an example of the convergence achieved for the 1 unit cell OS structure, increasing the number of tetrahedra from 31 634 to 36 407 per unit cell resulted in a maximum change of 0.18% in the S parameters. Further increasing the number of tetrahedra to 41 901 resulted in a maximum change in the S parameters of 0.12%. Since increasing the number of tetrahedra did not introduce notable changes in the S parameters an average of 37 000 tetrahedra per unit cell was used in the finite element simulations.

In each case perfect electric conductor (PEC) boundary conditions were employed on the z faces of the unit cell so that the electric field would be polarized along the strips, exciting their negative permittivity behavior. On the x faces,

[1]At the beginning of each iteration the mesh is refined in such a way that more tetrahedra are added to regions where the solved fields varied most between the two previous iterations.

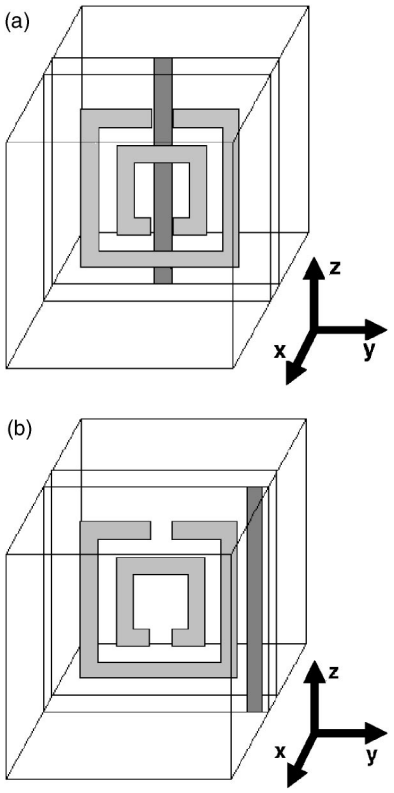

FIG. 2. (a) Opposite side (OS) structure. (b) Same side (SS) structure. In each case the metallic strip was 0.5 mm wide and the substrate was 0.5 mm thick with a dielectric constant of 3.02. The dimensions of the unit cell in the OS configuration were $2.5\times2.5\times2.5$ mm. In the SS configuration the dimensions were $4\times2.5\times2.5$ mm.

perfect magnetic conductor (PMC) boundary conditions were used so that the rings negative permeability behavior would be excited. In the y direction the unit cells were repeated 4 times such that transmission through a 4 unit cell structure was simulated. In the SS case the unit cell size was $4\times2.5\times2.5$ mm and in the OS case the unit cell size was $2.5\times2.5\times2.5$ mm. The reason for the difference in the x dimension will be discussed in the next section. The simulated transmission magnitude for the two structures is shown in Fig. 3. Solid (dashed) vertical lines indicate the regions of transition from RHM (LHM) to LHM (RHM) behavior. These lines will be discussed in the next section.

For both structures there is a peak in the transmission magnitude where both the real part of the electric permittivity and the real part of the magnetic permeability are expected to be negative. The peaks appear at 22.6 GHz and 22.75 GHz in the OS and SS cases, respectively. Because of these peaks, it seems reasonable to conclude that both configurations correspond to negative index regions, and hence LHM behavior. However, before making such conclusions, let us perform more thorough investigations and consider both the transmission phases and dispersion relations for these two cases.

III. TRANSMISSION PHASE

The sign of the effective index in a structure can be determined by considering the difference in the transmission

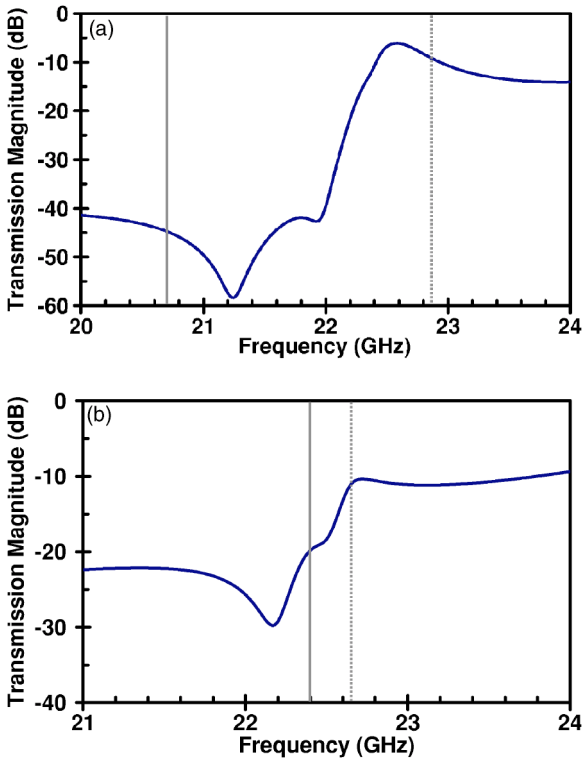

FIG. 3. Simulated transmission magnitude through 4 unit cell long (a) OS structure, and (b) the SS structure. Solid (dashed) vertical lines indicate the points at which the structures make transitions from RHM (LHM) to LHM (RHM) behavior.

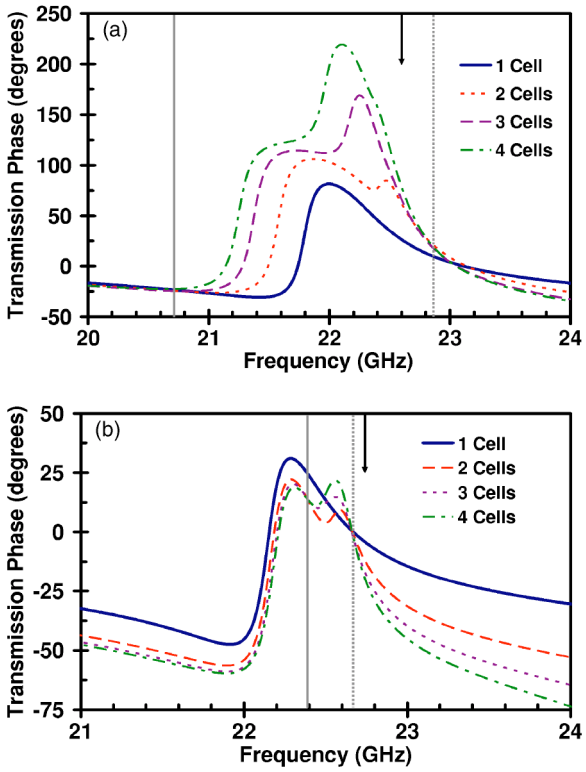

FIG. 4. (Color online) Transmission phase for propagation through 1, 2, 3, and 4 unit cells of (a) OS structure and (b) SS structure. Solid (dotted) vertical lines indicate the points at which the structures make transitions from RHM (LHM) to LHM (RHM) behavior. Arrows mark the locations of the transmission peaks from the corresponding OS or SS plots in Fig. 3.

phase for propagation through various lengths of the structure. For a medium with phase index $n(\omega)$ the transmission phase for propagation through a length L of the structure is given by

$$\phi = -n(\omega)L\frac{\omega}{c}, \tag{1}$$

where c is the speed of light in vacuum. For propagation through different lengths L_1 and L_2 of this medium the difference in the transmission phase is

$$\Delta\phi = -n(\omega)(L_2 - L_1)\frac{\omega}{c}. \tag{2}$$

For $L_2 > L_1$ this difference will be negative in RHM $[n(\omega) > 0]$, and positive in the LHM $[n(\omega) < 0]$ case. In other words, in the case of RHM the insertion phase of the longer structure will lie below that of the shorter structure, whereas the opposite is true for the LHM. The transmission phases for propagation through 1, 2, 3, and 4 unit cells of the SRR and SW configurations are shown in Fig. 4.[2] Regions where the structures make a transition from RHM to LHM behavior are marked by solid vertical lines. Dashed vertical lines indicate transitions from LHM to RHM behavior.

In Fig. 4(a) the phase difference $(\Delta\phi)$ is positive between 20.7 GHz (marked by a solid vertical line) and 22.85 GHz (marked by a dashed vertical line) for the two, three, and four unit cell structures, implying that the effective index is negative in this region. For the one unit cell case the phase difference is positive, and hence the index of refraction is negative, between 20.7 GHz and 22.95 GHz. In each case when the phase lines cross (at 22.85 GHz in the multiple unit cell case and at 22.95 GHz in the single unit cell case), the structures make a transition from LHM to RHM behavior. In Fig. 4(b) the phase difference is negative from 21 GHz to 22.4 GHz, so that the effective index is positive in this region. At 22.4 GHz the phase lines for the two, three, and four unit cell cases cross indicating a transition for these cases to LHM behavior (marked by a solid vertical line). The one unit cell case crosses and makes its transition to LHM behavior at 22.57 GHz. At 22.65 GHz all four cases return to RHM behavior (marked by a vertical dashed line). This difference in the behavior of the single and multiple unit cell cases is caused by the interactions between nearest neighbor SRRs. In the one unit cell case, the resonance region is due to an individual SRR which results in a single peak. On the other hand, the resonance regions in the two, three, or four unit cell cases are a result of both the individual SRR resonances and the interactions between nearest neighbor SRRs. Thus,

[2]Note that the transmission phase is invariant under 2π phase shifts. Hence, all phases in Fig. 4, are plotted in such a way that their initial value (20 GHz in the OS case and 21 GHz in the SS case) begins in the principle branch $(-180° < \theta < 180°)$. The phase at higher frequencies is then unwrapped starting from this point.

for the multiple unit cell cases there is a second peak in the phase plots which causes their LHM regions to differ from the single unit cell cases.

In Fig. 4(a), the location of the OS transmission peak from Fig. 3(a) is marked by an arrow. Similarly the SS transmission peak from Fig. 3(b) is marked by an arrow in Fig. 4(b). What is important to note is that in the OS case of Fig. 4(a) the LHM region contains the transmission peak, whereas in the SS case the transmission peak lies outside the LHM region. *Hence, in the passband, the OS structure is LHM and the SS structure is RHM*. Here, we have demonstrated that the transmission phase can be used to determine the handedness of a structure. However, using this transmission phase difference analysis is not always practical since it requires transmission data for several lengths of the structure. Therefore, it will be instructive to study the band diagrams (the dispersion plots) to further verify the above conclusions.

IV. DISPERSION DIAGRAMS

The dispersion characteristics of the SS and OS structures were also simulated using finite element method with the help of commercially available Ansoft-HFSS. The results were further verified using a finite difference time domain algorithm developed in-house. In the simulations, periodic boundary conditions were used on all faces of the unit cells shown in Fig. 2. On the x and z faces the phase was not varied, while in the y direction the phase was swept between 0° and 180°. The simulated dispersion plots are shown in Fig. 5 (solid lines). The light line in each structure was also simulated (dashed lines). When the mode resulting from the SRRs and SWs intersect the light line there is a coupling. Hence, for comparison, the dispersion plot was also calculated using an equivalent transmission line model for the OS case which does not take this coupling into account (dotted line).[3] It should be noted that this coupling was not present in the above transmission simulations because the light line mode is polarized such that its propagation was not allowed by the PEC and PMC boundaries.

Similar to any photonic crystal dispersion relation, the band diagrams in Figs. 5(a) and 5(b) are symmetric with respect to the origin (zero phase or equally zero propagation vector magnitude). Since for the case of one dimensional propagation considered here, the local derivative of the curves depicted above is the group velocity or equally the energy velocity (in the passband), then only branches marked (I) in Figs. 5(a) and 5(b) correctly predict the positive energy propagation within the two structures [12]. Note that in Fig. 5(a) while the local derivative (the group velocity) is positive within the branch I, the slope of the line joining the origin to any point on branch I is negative, indicative of a negative phase velocity. In other words, the mode described by branch I of Fig. 5(a) is a backward wave mode (positive group but negative phase velocity), and as such it indicates the existence of an effective negative index of refraction or LHM behavior for this configuration. On the other hand, the propagating mode of the SS structure depicted by branch I of Fig. 5(b) has both positive group and phase velocities, indicating the existence of a positive index of refraction or RHM behavior.[4] We also note that the concavity (the second derivative) of the propagating mode of Fig. 5(b) at the origin has an opposite sign as compared to the LHM bands, for which the curve is concave downward. These dispersion diagrams corroborate the results from Sec. III that, in the passband, the OS structure is a LHM and the SS structure is a RHM.

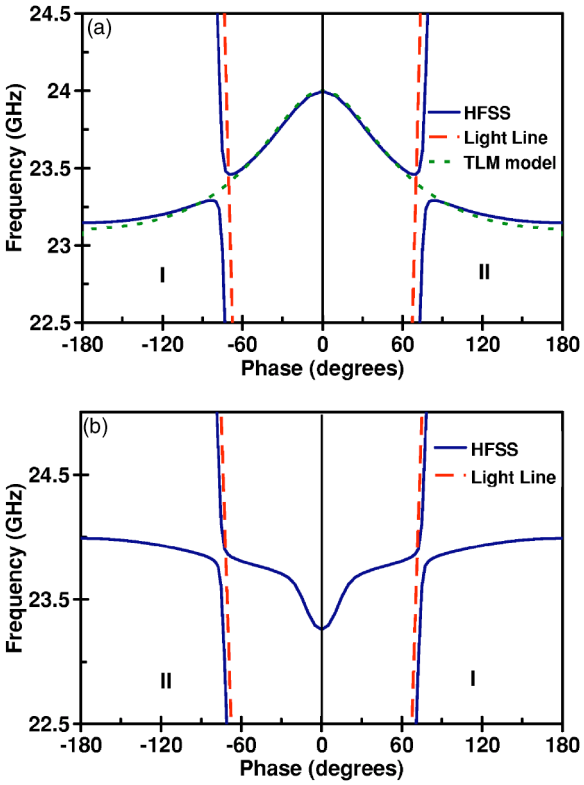

FIG. 5. (Color online) Dispersion plots for (a) OS structure and (b) SS structure. In the OS configuration the unit cell size was $2.5\times2.5\times2.5$ mm. The unit cell size was $4\times2.5\times2.5$ mm in the SS case.

The LHM and RHM character of these structures can also be seen by the manner in which they couple to the light line. In the OS case when the band corresponding to the SRRs and SWs intersects the light line the coupling results in the emergence of a stopband. This is characteristic of contradirectional coupling in which case the two interacting modes have counterpropagating wave vectors. In the SS structure, on the other hand, no stopband appears when the SRR and SW band intersects the light line, a characteristic of codirectional coupling in which the interacting waves are copropagating.

To further understand why the two configurations behave differently we must consider how the fields generated by the SRRs and SWs interact in each case. Figure 6 shows the

[3]This was done using a technique similar to that presented in [15].

[4]It should be noted that a negative group velocity (branch II), although physical, is only expected to occur in the anomalous dispersion region. Hence, in the passband, the propagating modes are described by the positive group velocity branches.

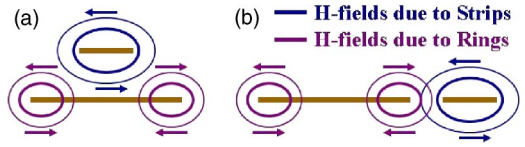

FIG. 6. (Color online) Magnetic fields resulting from the currents in the SRR and SW for (a) OS configuration and (b) SS configuration.

simulated magnetic fields due to the currents in the rings and strips for each configuration. The fields are shown in a plane perpendicular to the *z* axis and cut in the center of the cell. When the SRR and SW are on opposite sides of the substrate, as is the case for Fig. 6(a), there is little overlap between their magnetic fields, and the behavior of each component is not significantly affected by the presence of the other. On the other hand, when the SRR and SW are on the same side of the substrate [Fig. 6(b)] there is significant overlap between the fields. As a result, the original behavior of each component is not preserved and a new field pattern emerges. A similar argument was presented by Smith in [14].

At this point it is reasonable to ask the following question. Since the SS configuration exhibits LHM behavior in the stopband, can it be also made to display LHM behavior *in the passband under certain conditions*? In the following section, we will consider the effect of the unit cell size on the handedness of this configuration.

V. EFFECTS OF UNIT CELL SIZE

Consider an array of isolated SRRs. If the *x* dimension in Fig. 2(a) is reduced the resonators will be brought closer together thus enhancing the strength of the total resonance. This in effect will increase the negative value of the effective permeability. Consider now an array of isolated strip wires. Bringing the strip wires closer together in the *x* direction will cause an increase in the plasma frequency. As a result the negative value of the electric permittivity at a fixed frequency also increases. If the two structures are then combined (in either the SS or OS configuration) the same will still be true. That is, even though the structures interfere with one another differently, reducing the *x* dimension will strengthen their respective responses. From this argument we may expect that even the SS structure could be made to exhibit LHM behavior, if the unit cell size was decreased. Figure 7 shows several band diagrams for the SS structure obtained by varying the *x* dimension of the unit cell.

Similar to Fig. 5(b), in Fig. 7, when the unit cell is 4 mm long in the *x* direction (dotted) the slope of the dispersion curve is positive everywhere for the branch marked I, indicative of positive group and energy velocities. For this case, the RHM passband has a bandwidth of approximately 730 MHz. When the *x* dimension is decreased from 4 mm to 2.5 mm (dashed line) the passband is nearly flat with a bandwidth of 130 MHz. The slope of this band is negative for low phase values and slightly positive at higher phase values so that it is not clearly either LHM or RHM. However, further reduction of the unit cell size to 1.5 mm in the *x* direction, results in an LHM band with a 250 MHz bandwidth, with the correct behavior described by branch II of Fig. 7 (the solid line). Thus reducing the unit cell size allows the behavior of the structure to make a transition from RHM to LHM behavior, with the transition unit cell size being approximately 2.5 mm (where the passband was nearly flat).

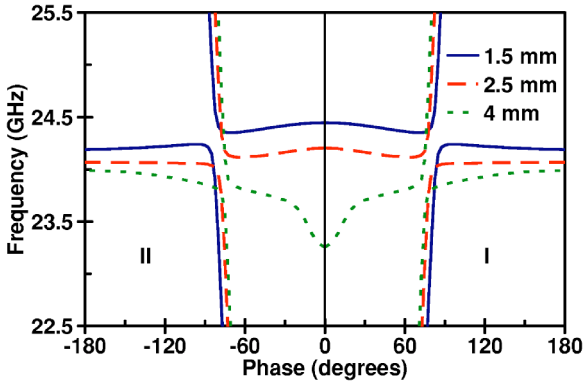

FIG. 7. (Color online) Dispersion curves for the SS structure. In each case the *y* and *z* dimensions of the unit cell were 2.5 mm and the *x* dimension was varied.

An examination of Fig. 7 also reveals an interesting point regarding the coupling of the SRR and SW band to the light line. In the 4 mm case, when the structure behaves as an RHM, the coupling does not result in the opening of a band gap. However, when the *x* dimension is reduced and the structure begins to exhibit LHM behavior, a band gap appears. In other words, we see a change from codirectional coupling (RHM-RHM) behavior at 4 mm to contradirectional coupling (RHM-LHM) behavior at 1.5 mm.

This analysis shows that both the OS and SS configurations of the SRRs and SWs can produce LHM behavior. But that in the SS case, because of the interference between the two components, the lattice spacing must be smaller than that of the OS case to obtain this behavior. Therefore the interference does not completely destroy the potential for LHM behavior, it merely weakens it.

VI. SUMMARY AND CONCLUDING REMARKS

The behavior of two SRR and SW configurations with the rings and wires on the same side and opposite side of the substrate was examined. It was shown that the existence of transmission peaks in the regions where the real parts of the electric permittivity and magnetic permeability are expected to be simultaneously negative is not sufficient evidence of LHM behavior. In order to properly determine the sign of the index, the insertion phase for propagation through several lengths of the structure is necessary. Alternately, the dispersion diagrams can be used to determine the sign of the index. In addition, it was shown that the unit cell size has a profound impact on the "handedness" of the structure and that the same side structure requires a smaller unit cell than the opposite side structure in order to exhibit the LHM behavior.

[1] V. G. Veselago, Sov. Phys. Usp. **10**, 509 (1968).
[2] J. B. Pendry, A. J. Holden, W. J. Stewart, and I. Youngs, Phys. Rev. Lett. **76**, 4773 (1996).
[3] J. B. Pendry, A. J. Holden, D. J. Robbins, and W. J. Stewart, IEEE Trans. Microwave Theory Tech. **47**, 2075 (1999).
[4] D. R. Smith, W. J. Padilla, D. C. Vier, S. C. Nemat-Nasser, and S. Schultz, Phys. Rev. Lett. **84**, 4184 (2000).
[5] R. A. Shelby, D. R. Smith, and S. Schultz, Science **292**, 77 (2001).
[6] G. V. Eleftheriades, A. K. Iyer, and P. C. Kremer, IEEE Trans. Microwave Theory Tech. **50**, 2702 (2002).
[7] M. Bayindir, K. Aydin, E. Ozbay, P. Markos, and C. M. Soukoulis, Appl. Phys. Lett. **81**, 120 (2002).
[8] O. F. Siddiqui, M. Mojahedi, and G. V. Eleftheriades, IEEE Trans. Antennas Propag. **51**, 2619 (2003).
[9] O. F. Siddiqui, S. J. Erickson, and G. V. Eleftheriades, IEEE Trans. Microwave Theory Tech. **52**, 1449 (2004).
[10] C. Caloz, H. Okabe, H. Iwai, and T. Itoh, *IEEE AP-S/URSI International Symposium*, San Antonio, TX, 2002, Vol. 2, p. 412.
[11] R. W. Ziolkowsky, IEEE Trans. Antennas Propag. **51**, 1516 (2003).
[12] J. F. Woodley, and M. Mojahedi, Phys. Rev. E **70**, 046603 (2004).
[13] R. A. Shelby, D. R. Smith, S. C. Nemat-Nasser, and S. Schultz, Appl. Phys. Lett. **78**, 489 (2001).
[14] C. M. Soukoulis, *Photonic Crystals and Light Localization in the 21st Century* (Kluwer Academic Publishers, Netherlands, 2001).
[15] G. V. Eleftheriades, O. Siddiqui, and A. K. Iyer, IEEE Microw. Wirel. Compon. Lett. **13**, 51 (2003).